Neurosci Bull October 1, 2015, 31(5): 561–571. http://www.neurosci.cn
DOI: 10.1007/s12264-014-1535-7

·Original Article·

Orientation selectivity in cat primary visual cortex: local and global measurement

Tao Xu[1,2], Hong-Mei Yan[1], Xue-Mei Song[2], Ming Li[3]

[1]*Key Laboratory for Neuroinformation of Ministry of Education, University of Electronic Science and Technology of China, Chengdu 610054, China*

[2]*Shanghai Institutes of Biological Sciences, Chinese Academy of Sciences, Shanghai 200031, China*

[3]*The Department of Automatic Control, College of Mechatronics and Automation, National University of Defense Technology, Changsha 410073, China*

Corresponding author: Xue-Mei Song. E-mail: xmsong@sibs.ac.cn

ABSTRACT

In this study, we investigated orientation selectivity in cat primary visual cortex (V1) and its relationship with various parameters. We found a strong correlation between circular variance (CV) and orthogonal-to-preferred response ratio (O/P ratio), and a moderate correlation between tuning width and O/P ratio. Moreover, the suppression far from the peak that accounted for the lower CV in cat V1 cells also contributed to the narrowing of the tuning width of cells. We also studied the dependence of orientation selectivity on the modulation ratio for each cell, which is consistent with robust entrainment of the neuronal response to the phase of the drifting grating stimulus. In conclusion, the CV (global measure) and tuning width (local measure) are significantly correlated with the modulation ratio.

Keywords: cat; orientation selectivity; tuning width; circular variance; primary visual cortex

INTRODUCTION

Orientation selectivity is an emergent property of neurons in the primary visual cortex (V1). In Hubel and Wiesel's feed-forward model, orientation selectivity arises from the alignment of the receptive fields of lateral geniculate nucleus (LGN) neurons presynaptic to each simple cell [1, 2]. However, the mechanisms underlying this selectivity are still under debate[3, 4]. There are essentially two models explaining the mechanisms of orientation selectivity, the feed-forward model that relies on the input from the LGN[1, 4-8] and the feedback model that relies on global inhibition to refine the selectivity to a weak bias provided by LGN input[3, 9-12]. The complexity of this issue is highlighted by recent studies explaining adaptation and learning-dependent orientation plasticity[13-15]. To address these issues, we studied the variation of orientation selectivity in cat V1 neurons.

Previous authors have studied the distribution of orientation tuning width[16, 17] in cat V1, measuring around the peak of the tuning function (local measure). The shape (aspect ratio) and number of receptive field subregions are major factors that affect the tuning width[18-20]. Orientation selectivity is also associated with a broader range of stimulus values (global measure). A study in macaque V1[21] reported that the orthogonal-to-preferred response ratio (O/P ratio) has a significant effect on the local and global orientation. Further studies[22, 23] have demonstrated that untuned suppression is crucial for generating highly orientation-selective cells in macaque V1. However, the impact of the O/P ratio and the suppression that are far from the optimal on orientation selectivity in cat V1 are unclear.

In this study, we measured orientation selectivity with drifting sinusoidal gratings in a large population of cat V1 neurons by using two different quantitative measures, the

tuning width and the circular variance (CV). The tuning width is a local measure of tuning around the preferred orientation, whereas the CV is a global measure of the tuning curve[24]. Furthermore, we compared our data in the cat primary visual cortex to the results in macaque V1.

MATERIALS AND METHODS

Animal Preparation

This study was performed in strict accordance with the recommendations in the Guideline for the Care and Use of Laboratory Animals from the National Institute of Health. The protocols were specifically approved by the Committee on the Ethics of Animal Experiments of the Shanghai Institute for Biological Sciences, Chinese Academy of Sciences (Permit Number: ER-SIBS-621001C).

Acute experiments were performed on 12 adult cats of both sexes (the same animals were also used for other parallel projects). Detailed descriptions of animal surgery, anesthesia, and recording techniques can be found in previous studies [25, 26]. Briefly, cats were anaesthetized prior to surgery with ketamine hydrochloride (30 mg/kg, i.v.), and then tracheal and venous cannulations were performed. After surgery, the animal was placed in a stereotaxic frame for performing a craniotomy and conducting neurophysiological procedures. During recording, anesthesia and paralysis were maintained with urethane (20 mg/kg/h) and gallamine triethiodide (10 mg/kg/h), and glucose (200 mg/kg/h) in Ringer's solution (3 mL/kg/h). Heart rate, electrocardiography, electroencephalography (EEG), end-expiratory CO_2, and rectal temperature were monitored continuously. Anesthesia was considered to be sufficient when the EEG indicated a permanent sleep-like state. Corneal, eyelid, and withdrawal reflexes were tested at appropriate intervals. Additional urethane was given immediately if necessary. The nictitating membranes were retracted and the pupils dilated. Contact lenses and additional corrective lenses were applied to focus the retina on a screen during stimulus presentation. At the end of the experiment, the animal was sacrificed by an overdose of barbiturate administered intravenously.

Single-Unit Recordings

Extracellular recordings were made from 168 neurons in the primary visual cortex of anaesthetized cats using tungsten-in-glass microelectrodes with exposed tips 5–10 μm in length, and 1–2 μm in diameter[27]. The electrodes were advanced into the cortex *via* a step-motor micro-drive (Narishige, Japan) vertically penetrating the cortical layers. The signal was amplified and band-pass filtered (0.3–10 kHz). Spikes were discriminated with a hardware window discriminator and time-stamped with an accuracy of 1 ms using our own data acquisition system. Only well-isolated cells satisfying strict criteria (fixed shape of action potential and the absence of spikes during the absolute refractory period) for single-unit recordings were collected for further analyses. Spikes were analyzed both during experiments and off-line using standard software packages and customized software written specifically for the purpose.

Visual Stimulation

Visual stimuli were generated by a Cambridge Systems VSG graphics board. The stimuli were patches of drifting sinusoidal gratings presented on a high-resolution monitor screen (40 cm × 30 cm) at a 100-Hz vertical refresh rate. The screen was kept at the same mean luminance as the stimulus patches (10 cd/m^2). The monitor was placed 57 cm from the cat's eyes. All recordings were from the area of cortex representing the central 10° of the visual field.

Procedures

When the single-cell action potentials were isolated, the basic attributes of the cell were measured, including orientation tuning, spatial and temporal frequency tuning, and response function. Each cell was stimulated monocularly *via* the dominant eye and characterized by measuring its response to conventional drifting sinusoidal gratings (the nondominant eye was occluded).

To locate the center of the classical receptive field (CRF), a narrow rectangular sine-wave grating patch (0.5°–1.0° wide × 3.0°–5.0° long at 40% contrast) was moved at successive positions along axes perpendicular or parallel to the optimal orientation of the cell, and the responses to its drift were measured. The grating was set at the optimal orientation and spatial frequency and drifted in the preferred direction at the optimal speed for individual recorded cells. The peak of the response profiles for both axes was defined as the center of the CRF.

We further confirmed that the stimulus was positioned in the center of the receptive field by performing an

occlusion test, in which a mask consisting of a circular blank patch and concentric with the CRF was gradually increased in size on a background drifting grating[28, 29]. If the center of the CRF was accurately determined, the mask curve would begin at the peak, and the response decrease as more of the receptive field was masked. If the curve obtained with the mask did not begin at the peak value, we considered the stimulus to be offset in relation to the receptive field center, and the position of the receptive field was reassessed.

Once the center of each cell's receptive field and the excitatory receptive field were identified, the orientation tuning of the neuron was re-measured with a 40% contrast grating at a fixed diameter of the CRF. The orientation tuning curves were obtained using angular steps of 15°. Contrast in the subsequent experiments was selected to elicit responses that reached ~90% of the saturation response for each cell with the center (CRF) contrast response function. Our contrast had a range of 20%–70% and a mode of 40%.

Modulation Ratio

The modulation ratio (MR) of the response to drifting sinusoidal gratings was calculated as MR = F1/F0, where F0 is the mean firing rate (DC) of the response and F1 the magnitude of the first harmonic of the response, corresponding to the temporal frequency of the grating (usually 3 Hz)[30].

Data Analysis and Statistics

To study orientation selectivity across a large population of neurons, it is useful to have a single number for each orientation-tuning curve that quantifies the degree of selectivity of the neuron. We used two different measures in our analysis. The first measure of selectivity was the CV of the response[24, 31, 32].

The CV was calculated from orientation tuning curve as follows. We measured the mean spike rate, r_k, in response to a grating drifting with angle θ_k. The angle θ_k ranged from 0° to 360° at equally-spaced intervals. From these data, the CV was defined as

$$CV = 1 - \left| \frac{\sum_k e^{i2\theta_k} r_k}{\sum_k r_k} \right|$$

The CV ranges from 1 for a completely non-orientated (flat) curve to 0 for an exceptionally oriented curve (zero response at all orientations except the preferred one).

The other measure of selectivity we used was the tuning curve width at half-height (WHH) as used previously[24,33]. The orientation tuning curves were fitted with the von Mises distribution:

$$R=R_o+R_1 e^{k[\cos 2\,(\mathrm{Ori}-\mathrm{Ori_p})-1]}$$

where R represents the response of the cell as a function of orientation (Ori), and R_1, R_0, $\mathrm{Ori_p}$, and k are free parameters[24]. We fit the raw data rather than the mean response at each orientation. The preferred orientation was defined as the peak of the fitted function ($\mathrm{Ori_p}$). The WHH of the fitted function was used to describe the tuning width, which was calculated as follows:

$$\mathrm{WHH}=\arccos[(\ln 0.5+k)/k]$$

The two measures, CV and WHH, provide different information about the shape of the tuning curve. CV is a global measure that is influenced by all of the data points on the tuning curve. WHH is a more local measure that depends on the shape of the curve around its peak and is not sensitive at all to the shape of the curve lying below 1/2 of the peak response.

The selectivity measures were calculated based on the mean spike rate of the neurons during the response to a visual stimulus. For simple cells, one could also define a similar measure with the first harmonic amplitude ($F1$) of the response. We did not subtract the spontaneous rate of the responses from the visually-driven responses before the calculation of CV and bandwidth. The statistical significance of the experimental data was evaluated using Student's *t*-test. In all analysis, P <0.05 was considered to be statistically significant.

RESULTS

We completed quantitative tests and analysis of 168 single neurons at eccentricities within 10° of the visual axis. The majority of the cells were recorded in superficial and intermediate layers.

WHH and CV in the V1 Population

There was a wide variation in orientation selectivity in cat V1 (Fig. 1). The mean WHH was 45.6 ± 26.9°. This was consistent with previous findings on tuning width in cat V1 by Watkins and Berkley[16] and Chen *et al.* [33], and was

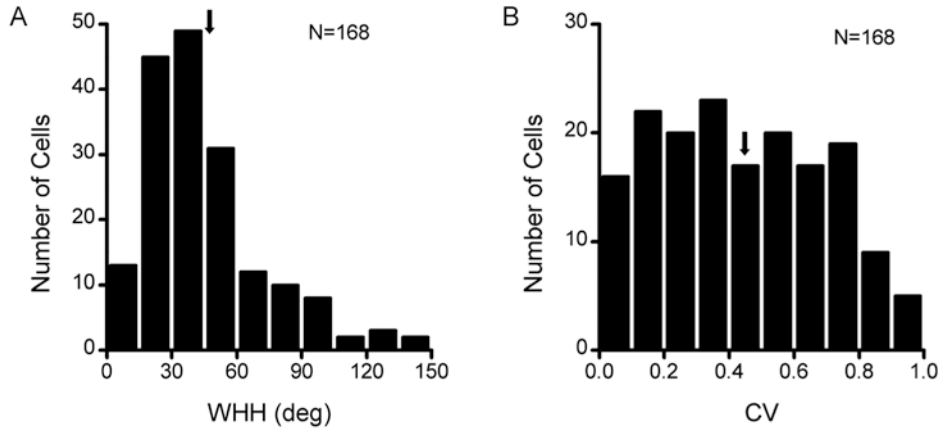

Fig. 1. Distribution of orientation selectivity in the V1 population. A. Distribution of WHH in the V1 population. The arrow indicates the mean WHH of cells. B. Distribution of CV for the V1 population. The arrow indicates the mean of CV of cells.

also similar to observations in the primary visual cortex of anaesthetized and alert monkeys[35, 36].

The distribution over the entire CV range was rather flat. The mean CV was 0.44 ± 0.26, generally consistent with the results in anaesthetized and alert monkey V1[21, 36].

To better understand the relationship between CV and WHH, we constructed a scatter plot of CV *versus* WHH (Fig. 2), and found that they were strongly correlated in cat V1 neurons (r = 0.60, P <0.001), also consistent with the results in anaesthetized and alert monkeys[21, 36].

The correlation was strong for CV <0.2 where WHHs were <40°; for larger CVs, the correlation was not so high. It is often the case that a narrow WHH is associated with many different CV values.

Orientation tuning curves based on spike counts for representative neurons are also displayed in Fig. 2. In

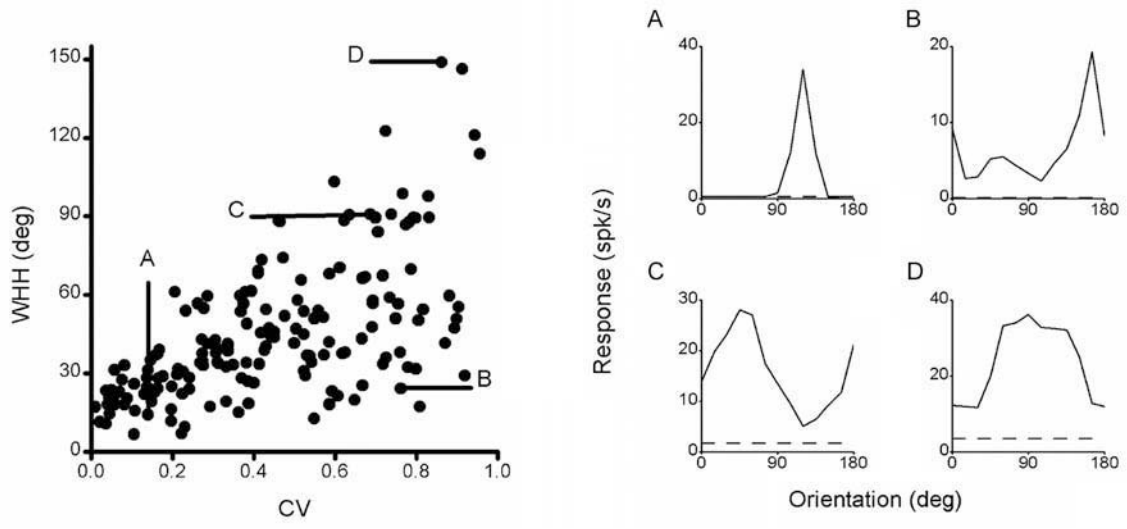

Fig. 2. Relationship between WHH and CV. Left panel, scatterplot of orientation WHH and CV for all neurons in the measured V1 population. A–D in the right panel, examples of individual tuning curves in different locations of the scatterplot. The x-axis represents stimulus orientation, from 0 to 180°. The y-axis is the response of the cell in spikes per second. The dashed line represents the spontaneous rate of firing.

some cases, the WHHs were similar, while the CVs were quite different (Fig. 2A, B), while in other cases the CVs were similar, but the WHHs were quite different (Fig. 2C, D). This disagreement between CV and WHH indicates that the two measures reflect different aspects of orientation selectivity: WHH depends on the local shape of the tuning curve around the peak, whereas CV weighs the global responses at all orientations.

Comparison of CV and WHH with the O/P Ratio

Previous experiments[21] in anaesthetized monkeys found that the O/P ratio is strongly correlated with CV, but less with bandwidth. Here, we compared the CV and WHH with the O/P ratio in cat V1. Scatter plots of the O/P ratio *versus* CV clearly showed that they were strongly correlated (r = 0.78, P <0.001) (Fig. 3A). Besides, there was a lower correlation (r = 0.47, P <0.001) between WHH and O/P ratio (Fig. 3B). These results suggest that the neuronal factors that cause low values of O/P ratios also lead to low values of CV, and these observations are similar to a report in anaesthetized monkeys[21]. Because of the finding that a low response far from the preferred orientation is crucial for a low CV, we next considered the effect of spontaneous activity on CV and WHH.

Relationship between Selectivity and Spontaneous Activity

There was a stronger correlation (r = 0.44, P <0.001)

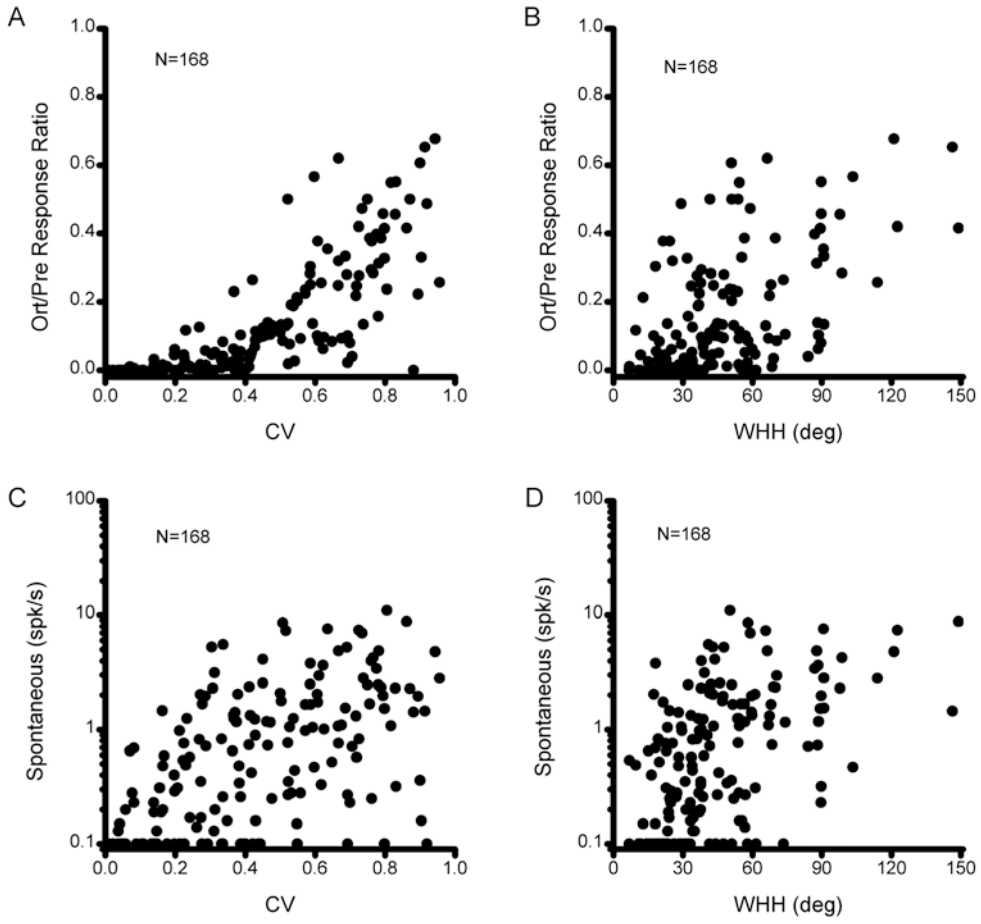

Fig. 3. Relationship between orientation selectivity and orthogonal/preferred orientation response ratio (O/P ratio) or spontaneous firing rate. A. Relationship between CV and O/P ratio. There is strong correlation between CV and O/P ratio in all samples. B. Relationship between WHH and O/P ratio. There is a moderate correlation between WHH and O/P ratio. C. Relationship between spontaneous firing rate and CV. D. Relationship between WHH and spontaneous firing rate.

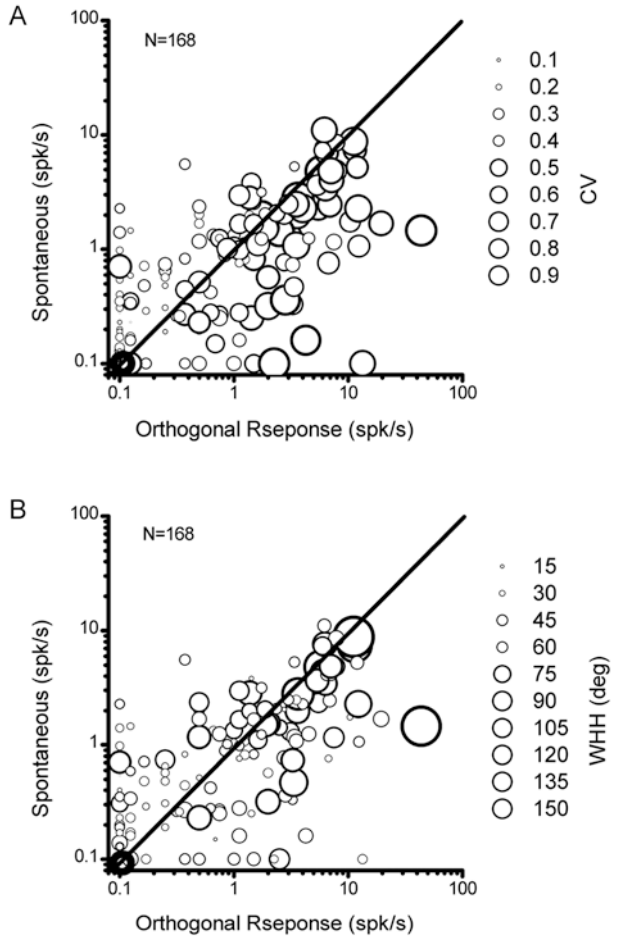

Fig. 4. Scatter plot for the orthogonal response (*x*-axis) *versus* the spontaneous firing rate (*y*-axis). The diagonal represents when the response at the orthogonal was equal to the spontaneous firing rate. A. CV as a function of spontaneous firing rate and the response at the orthogonal. The size of each data point corresponds to the CV of the tuning curve of the neuron as illustrated by the scale on the right. Points above the diagonal indicate that the cells have strong orientation selectivity, points below it indicate they have weak orientation selectivity. B. The size of each data point corresponds to the WHH of the tuning curve as illustrated by the scale on the right. The figure shows that cells with a narrow WHH are also located above the diagonal.

between spontaneous firing rate and CV (Fig. 3C) and a weaker correlation (r = 0.38, P <0.001) between spontaneous firing rate and WHH (Fig. 3D).

CV, WHH, Spontaneous Activity, and the Orthogonal Response

Additional analysis of the population data revealed that other factors determine orientation selectivity besides those that determine spontaneous firing rate. We plotted the orthogonal orientation firing rate *versus* the spontaneous firing (Fig. 4). Cells with zero spontaneous rates were plotted with *y*-coordinate 0.1. Cells with zero orthogonal response were plotted with an *x*-coordinate of 0.1. For this group of neurons (21 cells), both the spontaneous and orthogonal firing rates were zero.

Cells with low CVs were located above the diagonal, which confirms the role of inhibition of non-preferred orientation in the generation of high orientation selectivity (Fig. 4A). Cells with narrow tuning widths were also located above the diagonal, which implies that cortico-cortical suppression could also contribute to narrowing the tuning width (Fig. 4B).

Laminar Distribution of Orientation Selectivity of Neurons

Because of the uncertainty regarding the exact laminar position of our recording sites, we assigned laminar location by pooling those neurons estimated to be in the superficial layers (<600 μm), the intermediate layers (600–1200 μm), and the deep layers (>1200 μm)[37]. We illustrate the difference in laminar distribution focusing on the superficial and intermediate layers (because most of the cells were recorded in these layers). We found that the orientation WHH and CV were not uniformly distributed across the cortical layers, with a higher proportion of non-selective cells in the middle layers, and higher orientation selectivity in the superficial layers (Fig. 5).

A scatter plot of WHH *versus* depth in the cortex is shown in Fig. 5A and curves that depict descriptive statistical measures of the population data in Fig. 5B. The curves show the moving mean of WHH through the depth of the cortex using a window width of 100 μm. The curve was obtained by selecting, at each cortical depth, all of the data points from cells that were no more than 50 μm above and below and then computing the median of their WHHs. For WHH, there was a clear alteration of orientation selectivity with the layer of origin. Cells in middle layer had broader orientation tuning, while cells in the superficial layer showed sharper orientation tuning.

The orientation CV throughout all layers of cat V1, as the laminar scatter plot and statistical measures are shown in Fig. 5C and D. Although the WHH and CV of a single cell

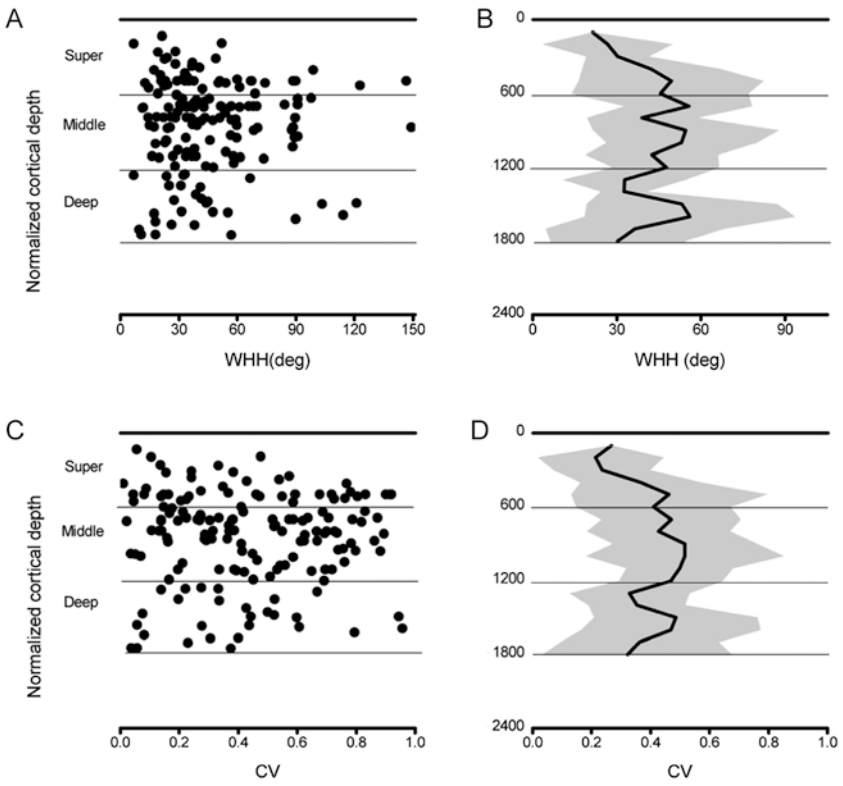

Fig. 5. Laminar analyses of WHH and CV for the V1 population. A. Plot of WHH against relative cortical depth. Each point represents a cell (*n* = 168). B. Statistical summary of the scatterplot data in A. The curve represents the mean bandwidth at different cortical depths. A window size of 100 μm, centered at each location, was used. C. Plot of CV against relative cortical depth. D. Statistical summary of the scatter plot data in C. Shaded area denotes ± SD in each bin. The cells located in layers >1800 μm are not shown because their number was small.

need not agree in their assessment of selectivity (Fig. 2), there was some concordance in the laminar patterns for the two different measures. Cells in the middle layers had higher CVs, while cells in the superficial layers had lower CVs.

Relationships of CV and WHH with MR

V1 neurons differ in the temporal modulation of the response to a drifting sinusoidal grating that is quantified by the F1/F0 ratio[30], with simple cells exhibiting values >1.0, and complex cells having ratios <1.0. However, it has been reported recently that the MR, when derived from the subthreshold membrane potential instead of from spike rate, is unimodally distributed[38]. So, we studied the correlation between measures of orientation selectivity and the MR (continuous distribution).

Interestingly, there were almost equal correlations of CV (r = –0.41, P <0.001) and WHH (r = –0.42, P <0.001) with the MR (Fig. 6A, B), different from the results in anaesthetized monkeys[21].

Relationships of O/P Ratio and Spontaneous Activity with MR

Because of the indication that the MR is crucial for CV and WHH, we next considered whether MR affects the O/P ratio or spontaneous activity. We found a negative correlation between the two values (r = –0.32, P <0.001) (Fig. 6C). There was also a negative correlation between spontaneous activity and MR (r = –0.36, P <0.001) (Fig. 6D).

DISCUSSION

Diversity

Our data point to the wide diversity of orientation selectivity

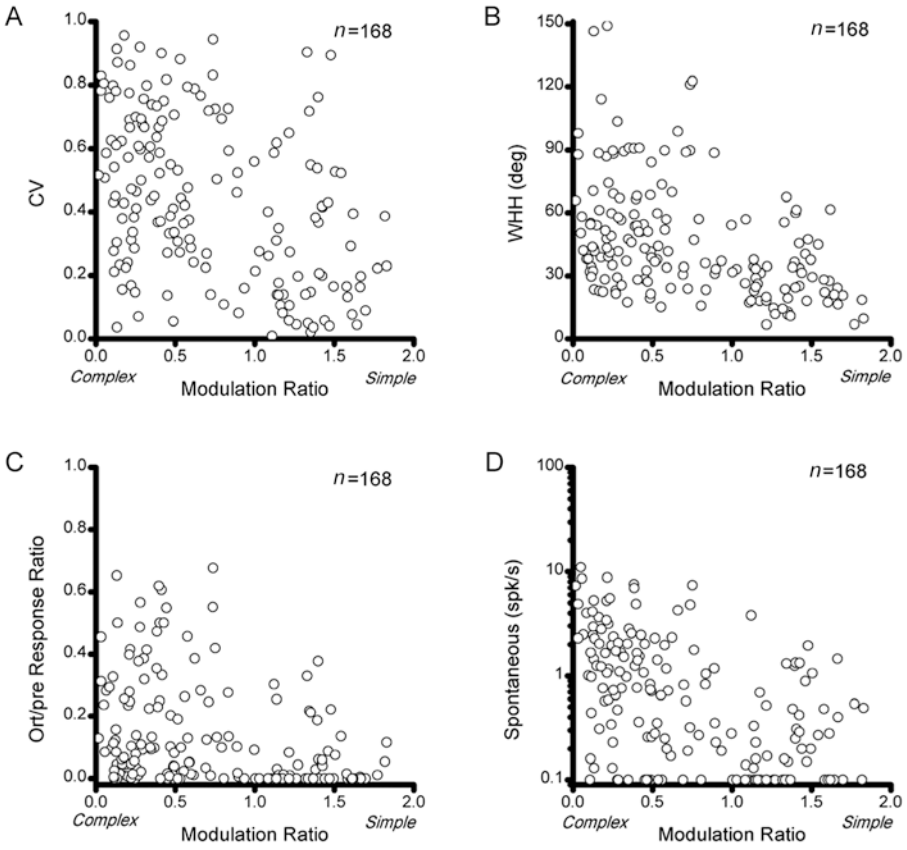

Fig. 6. Relationship between modulation ratio and CV, WHH, O/P ratio, or spontaneous rate. A, CV. B, WHH. C, O/P ratio. D, spontaneous rate.

in the population of cat V1 neurons, especially in the CV data, which are in agreement with the findings in V1 neurons in anaesthetized macaques[21].

The factors that control WHH are likely to be different from those determining CV. We found a stronger correlation between CV and the O/P ratio than WHH and the O/P ratio (Fig. 3). Thus, the diversity of the relative heights of the plateau and peak would strongly influence the diversity of CV, whereas the aspect ratio of the feedforward input might affect the variability of WHH[1, 18, 19].

A previous study reported that suppression far from the peak could account for low values of CV[21, 22]. In the present study, we showed that cortico-cortical suppression also contributed to the narrowing of the WHH (Fig. 4B).

MR and Orientation Selectivity

We found that cells with a low MR had a higher CV and WHH than those with a high MR (Fig. 6A, B). Neurons with a high MR are usually called simple cells, and those with a low MR are called complex cells. Previous studies have reported that simple cells have narrower tuning than complex cells in cat V1[16, 17], simple cells have a higher orientation selectivity index (OSI, equal to 1 − CV) than complex cells[36, 37], and the orientation tuning width is linearly related to the OSI (r = 0.54, P <0.001)[39]. These findings are similar to our results.

McLaughlin *et al*. (2000)[40] and Wielaard *et al*. (2001)[41] proposed that simple cells might receive more intracortical inhibition, which would be consistent with the lower spontaneous firing rate and orthogonal response rate. There is another possibility. A recent study based on the model[42] reported that well-defined LGN spike trains reduce the noise and elevate the response to the preferred stimulus. It is known that the relay cells are distributed nonrandomly in the LGN of cats and monkeys[43-47]. So the alignment of the receptive fields of relay cells in the LGN[1, 5, 7, 8] could also

explain the lower spontaneous response. However, there is perhaps only one possibility to explain the low spontaneous rate of complex cells: the strong cortico-cortical inhibition.

Comparisons with Other Species

The diversity of orientation selectivity in cat V1 reported here is generally consistent with the results from anaesthetized macaque V1[21]. Interestingly, CV and WHH were significantly correlated with the MR, which is different from the results in anaesthetized macaque V1[21]. Our results showed that the neurons of high MR (simple cells) had significantly narrower WHH than the neurons of low MR (complex cells) in cat V1 (Fig. 6B).

A type of simple-cell-like, orientation-tuned inhibitory neuron (driven by the thalamus)[48] is the main inhibitory component to form the orientation selectivity of simple cells in cat V1. Although both tuned and global sources of inhibition contribute to the orientation dynamics in monkeys[49], only the interneuron with bordering tuning for orientation has been reported in monkeys[50]. Moreover, in recent years, studies[3, 22, 23] have mainly focused on global inhibition (driven by the cortex) which has a crucial influence on the generation of highly orientation-selective cells (global measure for selectivity - CV) in monkey V1, and the effect of tuned suppression narrowing bandwidth in the most highly tuned cells has seldom been studied[49].

Using genetic and imaging tools, recent evidence for orientation selectivity in mouse V1 has not found inhibitory neurons with simple-cell-like RFs, but has found interneurons with complex-cell-like RFs and hardly any orientation selectivity[51]. More evidence shows that the push-pull circuit (in cat V1)[1, 52, 53] cannot be a major synaptic mechanism underlying simple RFs in mouse V1 and the inhibitory circuit (driven by cortex) may contribute in a different way than in cat V1 to form orientation selectivity in simple cells[51, 54, 55].

Highly orientation-selective neurons (simple cells in layer 4) are already present in the first stage of cortical processing in cat V1[56], and their generation of orientation tuning relies on a substantial feed-forward mechanism[1, 7, 57, 58]. Although this is true for other carnivores[59], it is not a universal rule. For example, cells in layer 4 of the tree shrew cortex are not tuned to stimulus orientation[60], but the orientation selectivity in layer 2/3 of the tree shrew appears to depend on the axial bias in its feed-forward input from layer 4, further refined by the intracortical circuits[61].

In primates, the parvo- and magno-cellular pathways remain separate in the LGN. Parvo- and magno-cellular relay cells target different sub-laminae of cortical layer 4C[62]. Cortical cells in the magnocellular stream have orientation-selective responses[63], similar to the organization in cats. However, the poor orientation tuning in the parvocellular stream may be similar to the organization in the tree shrew[62].

In future work, it will be necessary to analyze the inhibitory and excitatory input to cells in layer 4C of primates. Perhaps many of the same arguments that we make here for the cat visual cortex might apply to the primate visual cortex.

ACKNOWLEDGMENTS

This work was supported by the National Basic Research Development Program of China (2013CB329401), the National Natural Science Foundation of China (91420105, 61105116, 91120013, and 90820301), and Shanghai Municipal Committee of Science and Technology (088014158 and 098014026). We thank Dr. D. A. Tigwell for comments on the manuscript and X. Z. Xu for technical assistance. We also thank Dr. L. Wang and Y. C. Cai for help with the stimulus and analysis programs.

Received date: 2014-11-23; Accepted date: 2015-04-13

REFERENCES

[1] Hubel DH, Wiesel TN. Receptive fields, binocular interaction and functional architecture in the cat's visual cortex. J Physiol 1962, 160: 106–154.

[2] Hubel DH, Wiesel TN. Receptive fields and functional architecture of monkey striate cortex. J Physiol 1968, 195: 215–243.

[3] Shapley R, Hawken M, Ringach DL. Dynamics of orientation selectivity in the primary visual cortex and the importance of cortical inhibition. Neuron 2003, 38: 689–699.

[4] Priebe NJ, Ferster D. Inhibition, spike threshold, and stimulus selectivity in primary visual cortex. Neuron 2008, 57: 482–497.

[5] Chapman B, Zahs K, Stryker MP. Relation of cortical cell orientation selectivity to alignment of receptive fields of the geniculocortical afferents that arborize within a single orientation column in ferret visual cortex. J Neurosci 1991, 11: 1347–1358.

[6] Nelson S, Toth L, Sheth B, Sur M. Orientation selectivity of

cortical neurons during intracellular blockade of inhibition. Science 1994, 265: 774–777.

[7] Ferster D, Chung S, Wheat H. Orientation selectivity of thalamic input to simple cells of cat visual cortex. Nature 1996, 380: 249–252.

[8] Zhan X, Shou T. Anatomical evidence of subcortical contributions to the orientation selectivity and columns of the cat's area 17. Neurosci Lett 2002, 324: 247–251.

[9] Vidyasagar TR. Contribution of inhibitory mechanisms to the orientation sensitivity of cat dLGN neurones. Exp Brain Res 1984, 55: 192–195.

[10] Eysel UT, Shevelev LA, Lazareva NA, Sharaev GA. Orientation tuning and receptive field structure in cat striate neurons during local blockade of intracortical inhibition. Neuroscience 1998, 84: 25–36.

[11] Somers DC, Nelson SB, Sur M. An emergent model of orientation selectivity in cat visual cortical simple cells. J Neurosci 1995, 15: 5448–5465.

[12] Sompolinsky H, Shapley R. New perspectives on the mechanisms for orientation selectivity. Curr Opin Neurobiol 1997, 7: 514–522.

[13] Dragoi V, Sharma J, Miller EK, Sur M. Dynamics of neuronal sensitivity in visual cortex and local feature discrimination. Nat Neurosci 2002, 5: 883–891.

[14] Felsen G, Shen YS, Yao H, Spoor G, Li C, Dan Y. Dynamic modification of cortical orientation tuning mediated by recurrent connections. Neuron 2002, 36: 945–954.

[15] Tian Y, Liang SS, Yao DZ. Attentional orienting and response inhibition: insights from spatial-temporal neuroimaging. Neurosci Bull, 2014, 30: 141–152.

[16] Watkins DW, Berkley MA. The orientation selectivity of single neurons in cat striate cortex. Exp Brain Res 1974, 19: 433–446.

[17] Heggelund P, Albus K. Orientation selectivity of single cells in striate cortex of cat: the shape of orientation tuning curves. Vision Res 1978, 18: 1067–1071.

[18] Movshon JA, Thompson ID, Tolhurst DJ. Spatial summation in the receptive fields of simple cells in the cat's striate cortex. J Physiol 1978, 283: 53–77.

[19] Jones L, Palmer LA. An evaluation of the two-dimensional Gabor filter model of simple receptive fields in cat striate cortex. J Neurophysiol 1987, 58: 1233–1258.

[20] Sasaki KS, Ohzawa I. Internal spatial organization of receptive fields of complex cells in the early visual cortex. J Neurophysiol 2007, 98: 1194–1212.

[21] Ringach DL, Shapley RM, Hawken MJ. Orientation selectivity in macaque V1: diversity and laminar dependence. J Neurosci 2002b, 22: 5639–5651.

[22] Ringach DL, Bredfeldt CE, Hawken MJ, Shapley R. Suppression of neural responses to nonoptimal stimuli correlates with tuning selectivity in macaque V1. J Neurophysiol 2002a, 87: 1018–1027.

[23] Xing D, Ringach DL, Hawken MJ, Shapley RM. Untuned suppression makes a major contribution to the enhancement of orientation selectivity in macaque V1. J Neurosci 2011, 31: 15972–15982.

[24] Swindale NV. Orientation tuning curves: empirical description and estimation of parameters. Biol Cybern 1998, 78: 45–56.

[25] Chen K, Song XM, Li CY. Contrast-dependent variations in the excitatory classical receptive field and suppressive nonclassical receptive field of cat primary visual cortex. Cereb Cortex 2013, 23: 283–292.

[26] Xu T, Wang L, Song XM, Li CY. The detection of orientation continuity and discontinuity by cat V1 neurons. Plos One 2013, 8(11): e79723.

[27] Li CY, Xu XZ, Tigwell D. A simple and comprehensive method for the construction, repair and recycling of single and double tungsten microelectrodes. J Neurosci Methods 1995, 57: 217–220.

[28] Levitt JB, Lund JS. The spatial extent over which neurons in macaque striate cortex pool visual signals. Vision Neurosci 2002, 19: 439–452.

[29] Song XM, Li CY. Contrast-dependent and contrast-independent spatial summation of primary visual cortical neurons of the cat. Cereb Cortex 2008, 18: 331–336.

[30] Skottun BC, DeValois RL, Grosof DH, Movshon JA, Albrecht DG, Bonds AB. Classifying simple and complex cells on the basis of response modulation. Vision Res 1991, 31: 1079–1086.

[31] Worgotter F, Eysel UT. Quantification and comparison of cell properties in cat's striate cortex determined by different types of stimuli. Biol Cybern 1987, 57: 349–355.

[32] Leventhal AG, Thompson KG, Liu D, Zhou Y, Ault SJ. Concomitant sensitivity to orientation, direction, and color of cells in layers 2, 3, and 4 of monkey striate cortex. J Neurosci 1995, 15: 1808–1818.

[33] Chen G., Dan Y., and Li C.Y. Stimulation of non-classical receptive field enhance orientation selectivity in the cat. J Physiol 2005, 564: 233–243.

[34] Leventhal AG, Hirsch HV. Receptive-field properties of neurons in different laminae of visual cortex of cat. J Neurophysiol 1978, 41: 948-962.

[35] Schiller PH, Finlay BL, Volman SF. Quantitative studies of single cell properties in monkey striate cortex. II. Orientation specificity and ocular dominance. J Neurophysiol 1976, 39: 1320–1333.

[36] Gur M, Kagan I, Snodderly DM. Orientation and direction electivity of neurons in V1 of alert monkeys: functional relationships and laminar distributions. Cereb Cortex 2005, 15: 1207–1221.

[37] Schummers J, Cronin B, Wimmer K, Stimberg M, Martin R, Obermayer K, Koerding K, Sur M. Dynamics of orientation tuning in cat V1 neurons depend on location within layers and orientation maps. Frontier in Neurosci 2007, 1: 145–159.

[38] Priebe NJ, Mechler F, Carandini M, Ferster D. The contribution of spike threshold to the dichotomy of cortical simple and complex cells. Nat Neurosci 2004, 7: 1113–1122.

[39] Liu YJ, Hashemi-Nezhad M, Lyon DC. Dynamics of extraclassical surround modulation in three types of V1 neurons. J Neurophysiol 2011, 105: 1306–1317.

[40] McLaughlin D, Shapley R, Shelley M, Wielaard DJ. A neuronal network modelof macaque primary visual cortex (V1): orientation selectivity and dynamics in the input layer 4C. Proc Natl Acad Sci USA 2000, 97: 8087–8092.

[41] Wielaard DJ, Shelley M, McLaughlin D, Shapley R. How simple cells are made in a nonlinear network model of the visual cortex. J Neurosci 2001, 21: 5203–5211.

[42] Lin IC, Xing DJ, Shapley R. Integrate-and-fire vs Poisson models of LGN input to V1 cortex: noisier inputs reduce orientation selectivity. J Comput Neurosci 2012, 33: 559–572.

[43] Lee BB, Creutzfeldt OD, Elepfandt A. The responses of magno- and parvocellular cells of the monkey's lateral geniculate body to moving stimuli. Exp Brain Res 1979, 35: 547–557.

[44] Kaplan E, Shapley RM. X and Y cells in the lateral geniculate nucleus of macaque monkeys. J Physiol 1982, 330: 125–143.

[45] Vidyasagar TR, Urbas JV. Orientation sensitivity of cat LGNd neurones with and without inputs from visual cortical areas 17 and 18. Exp Brain Res 1992, 46: 157–169.

[46] Shou T, Ruan D, Zhou Y. The orientation bias of LGN neurons shows topographic relation to area centralis in the cat retina. Exp Brain Res 1986, 64: 233–236.

[47] Shou T, Leventhal AG. Organized arrangement of orientation sensitive relay cells in the cat's dorsal lateral geniculate nucleus. J Neurosci 1989, 9: 4287–4302.

[48] Hirsch JA, Martinez LM, Pillai C, Alonso JM, Wang Q, Sommer FT. Functionally distinct inhibitory neurons at the first stage of visual corticalprocessing. Nat Neurosci 2003, 6: 1300–1308.

[49] Ringach, DL, Hawken, MJ, Shapley, RM. Dynamics of orientation tuning in macaque V1: the role of global and tuned suppression. J Neurophysiol 2003, 90: 342–352.

[50] Sato H, Katsuyama N, Tamura H, Hata Y, Tsumoto T. Mechanisms underlying orientation selectivity of neurons in the primary visual cortex of the macaque. J Physiol 1996, 494: 757–771.

[51] Liu BH, Li P, Li YT, Sun YJ, Yanagawa Y, Obata K, Zhang LI, TaoHW. Visual receptive field structure of cortical inhibitory neurons revealed by two-photon imaging guided recording. J Neurosci 2009, 29: 10520-10532.

[52] FersterD. Spatially opponent excitation and inhibition in simple cells of the cat visual cortex. J Neurosci 1988, 8: 1172–1180.

[53] Hirsch JA, Alonso JM, Reid RC, Martinez LM. Synaptic integration in striate cortical simple cells. J Neurosci 1998, 18: 9517–9528.

[54] Liu BH, Li P, Sun YJ, Li YT, Zhang LI, Tao HW. Intervening inhibition underlies simple-cell receptive field structure in visual cortex. Nat Neurosci 2010, 13: 89–96.

[55] Tan AY, Brown BD, Scholl B, Mohanty D, Priebe NJ. Orientation selectivity of synaptic Input to neurons in mouse and cat primary visual cortex. J Neurosci 2011, 31: 12339–12350.

[56] Hirsch JA, Martinez LM. Laminar processing in the visual cortical column. Curr Opin Neurobiol 2006, 16: 377–384.

[57] Chung S, Ferster D. Strength and orientation tuning of the thalamic input to simple cells revealed by electrically evoked cortical suppression. Neuron 1998, 20: 1177–1189.

[58] Lampl L, Anderson JS, Gillespie D, Ferster D. Prediction of orientation selectivity from receptive field architecture in simple cells of cat visual cortex. Neuron 2001, 30: 263–274.

[59] Usrey WM, Sceniak MP, Chapman B. Receptive fields and response properties of neurons in layer 4 of ferret visual cortex. J Neurophysiol 2003, 89: 1003–1015.

[60] Chisum HJ, Mooser F, Fitzpatrick D. Emergent properties of layer 2/3 neurons reflect the collinear arrangement of horizontal connections in tree shrew visual cortex. J Neurosci 2003, 23: 2947–2960.

[61] Mooser F, Bosking WH, Fitzpatrick D. A morphological basis for orientation tuning in primary visual cortex. Nat Neurosci 2004, 7: 872-879.

[62] Callaway EM. Structure and function of parallel pathways in the primate early visual system. J Physiol 2005, 566: 13–19.

[63] Bullier J, Henry GH. Ordinal position and afferent input of neurons in monkey striate cortex. J Comp Neurol 1980, 193: 913–935.